
Aircraft Noise – Aeroacoustics: Paper ICA2016–191

Parsimonious approaches for the laboratory synthesis of wall-pressure excitations

Cédric Maury^(a), Teresa Bravo^(b)

^(a) Laboratory of Mechanics and Acoustics, Marseille, France, cedric.maury@centrale-marseille.fr

^(b) Consejo Superior de Investigaciones Científicas, Madrid, Spain, teresa.bravo@csic.es

Abstract

The experimental synthesis of acoustic or aerodynamic wall-pressure excitations over industrial structures, for instance an aircraft sidewall or a car window, is a cost-efficient approach in order to optimise the insulating performance of these structures under real-life forcing generated in a controlled environment. Several strategies like inverse filtering in the spatial or wavenumber domains, holophonic or holographic reproductions, have proved to be successful for the laboratory synthesis of an acoustic diffuse field. But they required a prohibitive number of control sources for the real-time synthesis of sub-wavelength scales such as those associated with the wall-pressures induced by a Turbulent Boundary Layer (TBL). The present study compares the performance of several strategies for a direct reproduction of TBL excitations, independently of the test panel physical properties and with a reasonable number of sources. A first approach, the focused synthesis, uses spatial windowing to reduce the surface over which the TBL is reproduced, thereby enlarging the range of synthesized wavenumbers in the subsonic domain, if possible beyond the convective ridge. The two other approaches aim at synthesizing a reduced-rank approximation to either the target TBL correlation function or the source-fields acoustical transfers. The efficiency of these methods will be examined in terms of both the reproduction accuracy and the required number of sources that can be used to achieve the synthesis over a broad frequency range.

Keywords: sound field synthesis, turbulent boundary layer

Parsimonious approaches for the laboratory synthesis of wall-pressure excitations

1 Introduction

It appeared for several years a growing interest for the design of industrial and academic ground testing facilities able to reproduce in a controlled environment the effect of real-life forcing on structures using a network of suitably driven mechanical or acoustic actuators [1-4]. These approaches provide a cost-efficient methodology that allows parametric optimization of the acoustic performance of insulating structures under real-life loading pressures [5]. In particular, the laboratory synthesis of wall-pressure fluctuations such as those induced by a Turbulent Boundary Layer (TBL) on sidewall fuselage panels would allow to develop at the design stage potential solutions in order to reduce the transmission of this aerodynamic noise. It is known to be predominant in aircraft cabins under cruise conditions between 500 Hz and 2 kHz [6], with the highest sound pressure levels between 600 Hz and 800 Hz [7].

A number of experimental [8-14] studies have been undertaken for a direct reproduction of the statistical properties of random wall-pressure fluctuations over a transmitting panel with relevance to the aeronautical, automotive and building sectors. A planar array of 4×4 near-field loudspeakers, when suitably driven, was able to synthesize an Acoustic Diffuse Field (ADF) over a transmitting panel below the Schroeder frequency of the source room transmission suite [10]. This array system was also used to reproduce the sound power radiated by a TBL-excited panel up to its aerodynamic coincidence frequency [11]. In either cases, the loudspeakers were driven by optimal signals able to equalize for all the source-field transfer functions that occur between the source and the reproduction surfaces [8-9]. Direct approaches such as Wave Field Synthesis [12] or Direct Near-Field Acoustical Holography [13] have also been investigated for the real-time reproduction of supersonic TBL and ADF wall-pressures. They do not require, in either case, inversion of the source-field propagation operator. The inverse and direct approaches were able to reproduce correlation lengthscales larger than the acoustic wavelength, e.g. an ADF or a supersonic TBL, using a reasonable number of acoustic sources, at least two per wavelength. However, in order to reproduce a subsonic TBL, these studies found a criterion of at least 4 sources per unit trace of the smallest wavelength to be generated over the test panel, assuming it is equal to the convective lengthscale $\Lambda = U_c / \omega$ where ω is the angular frequency and $U_c \approx 0.6U_\infty$ is the flow convection velocity, with U_∞ the free-stream velocity. Hence, synthesizing a high speed TBL at Mach 0.66 using a near-field array of 4×4 loudspeakers shows acceptable accuracy only up to about 200 Hz [10] due to the inability of such a small number of sources to reproduce the exponential decay of the TBL correlation area. A synthetic antenna made up of a volume velocity source that can be sequentially located at an arbitrary number of positions over the source plane was able to reconstruct, after post-processing, the vibrating response of a panel excited by a TBL [14], albeit not in real-time.

These studies confirm that the main limiting factor for TBL synthesis is the prohibitively large number of sources required to approximate the TBL correlation area that typically decays as ω^{-2} when the frequency increases. For instance, an array of 286 sources would be required for real-time synthesis of a TBL up to 1.5 kHz over a fuselage panel. This would be unpractical as this necessitates small-sized loudspeakers with reduced performance in the low frequency range. Synthesizing the TBL-induced panel velocity, which is spatially more correlated than the TBL excitation, would only require an array of 60 sources [11], but the simulation process would then be panel-dependent and would require a preliminary modal analysis of each test panel.

In the present study, parsimonious approaches are investigated in order to reduce the required number of sources for a direct synthesis of wall-pressure excitations correlated over subwavelength scales such as a TBL. First, a focused synthesis approach is presented in Section 2 in which the simulation surface is spatially windowed, thereby extending in the wavenumber domain the support of the TBL towards higher subsonic wavenumbers, if possible beyond the convective wavenumber $k_c = \omega/U_c$. Sections 3 and 4 present parsimonious approaches in which an eigenanalysis is performed of either the wall-pressure Cross-Spectral Density (CSD) or the source-field radiative transfers, respectively. The efficiency of these approaches will be compared and assessed in terms of the frequency bandwidth over which the TBL CSD properties are accurately reproduced given a reasonable number of sources.

2 Focused synthesis of a TBL

2.1 Methodology

One considers a planar near-field array of loudspeakers, of size $A \times B$, located at a standoff distance h from a test panel over which the statistical properties of the TBL-induced wall-pressures, $\tilde{\mathbf{d}}$, are reproduced. The loudspeakers are driven in order to synthesize these target wall-pressures over a grid of evenly distributed microphones located close to the test panel and of size $a \times b$, lower than the size of the source array, as shown in Figure 1.

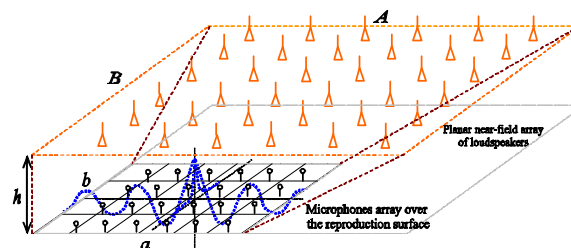


Figure 1: Focused near-field array of loudspeakers driven to reproduce a TBL over a simulation surface of size the quarter of the loudspeaker array

A matrix of control filters, \mathbf{W} , is calculated that provides drive signals to the source array. These signals are such that the microphones outputs, $\tilde{\mathbf{y}}$, are statistically equivalent to those induced by a TBL, $\tilde{\mathbf{d}}$. The cost function is then to minimize, in the mean-square sense, the vector of

error signals, $\tilde{\mathbf{e}}$, between the desired and generated pressure output signals. After some algebra, one obtains the following expressions for the optimum control filter matrices associated to a regular (resp. focused) TBL synthesis:

$$\mathbf{W}_{\text{opt},d} = \mathbf{G}^\dagger \mathbf{D}, \quad (1)$$

$$\mathbf{W}_{\text{opt},f} = \mathbf{G}_f^\dagger \mathbf{D}_f, \quad (2)$$

where \mathbf{D} (resp. \mathbf{D}_f) is a generating filter matrix obtained from an eigen-decomposition of the CSD matrix $\mathbf{S}_{dd} = \mathbb{E}[\tilde{\mathbf{d}}\tilde{\mathbf{d}}^H] = \mathbf{D}\mathbf{D}^H$ (resp. $\mathbf{S}_{ff} = \mathbf{D}_f\mathbf{D}_f^H$ when focused synthesis is performed over the reduced surface $a \times b$ with $a < A$ and $b < B$). \mathbf{G} (resp. \mathbf{G}_f) is the plant transfer matrix between the sources and the microphones distributed over the surface $A \times B$ close to the test panel (resp. a subset of the microphones spread over the surface $a \times b$ with $a < A$ and $b < B$).

For a high-speed fully-developed subsonic TBL, the matrix \mathbf{S}_{dd} is readily given by a Corcos model that describes the second order statistics of the TBL wall-pressures between two microphones located a distance $r = \sqrt{r_x^2 + r_y^2}$ apart from each other [15] :

$$S_{dd}(r; \omega) = S_0(\omega) e^{-|r_x|/L_x} e^{-|r_y|/L_y} e^{-j\omega r_y/U_c}, \quad (3)$$

where L_x and L_y are respectively the spanwise and streamwise correlation lengths. They decay with the frequency as $L_{\{x,y\}} = \alpha_{\{x,y\}} U_c / \omega$ with α_x and α_y empirical coefficients taken to be respectively 1.2 and 8. $S_0(\omega)$ is the auto power spectrum of the TBL wall-pressures assumed to be homogeneous over the test panel. The 2D spatial Fourier transform of $S_{dd}(r_x, r_y; \omega)$ is denoted $K_{dd}(k_x, k_y; \omega)$.

2.2 Simulation results

The target wall-pressures are reproduced by a near-field array of 8×8 volume velocity sources, evenly distributed over a source plane of size $0.84 \text{ m} \times 0.84 \text{ m}$ with a separation distance $\delta_A = \delta_B = 0.12 \text{ m}$, which is also the standoff distance h between the source and the reproduction planes in order to lower the plant matrices condition numbers. When performing a regular synthesis, the TBL is reproduced over a grid of size $0.92 \text{ m} \times 0.74 \text{ m}$ constituted of 35×27 microphones uniformly spread over the simulation surface, so that the spatial resolution is given by $\delta_a = 0.027 \text{ m}$ and $\delta_b = 0.028 \text{ m}$. These dimensions correspond to those of an experimental set-up currently installed in the LMA semi-anechoic room for the synthesis of random wall-pressures. Focusing the synthesis is equivalent to reproduce the TBL wall-pressures over a sub-domain of the initial simulation surface, say a quarter of the initial surface made up of a grid of size $0.46 \text{ m} \times 0.37 \text{ m}$ made up of 18×14 microphone positions uniformly

distributed and with the same spatial resolution as for a regular synthesis. The 64 drive signals are calculated in order to reproduce the CSD given by Eq. (3) and induced by a high-speed subsonic TBL with flow free-stream velocity $U_\infty = 255 \text{ m}\cdot\text{s}^{-1}$.

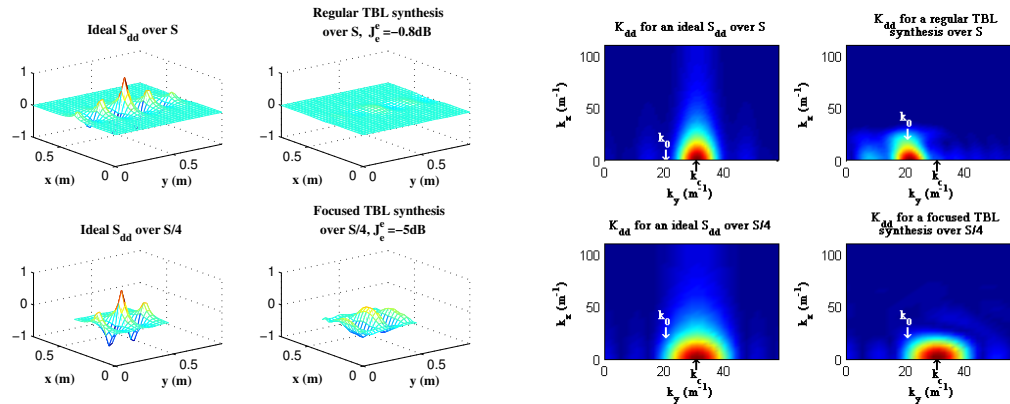


Figure 2: Focused synthesis of a high-speed subsonic TBL and its effect at 1 kHz in the spatial (left) and in the wavenumber domains (right)

Figure 2 (left) clearly shows that a near-field array of 8×8 suitably driven sources is not able to reproduce the intercorrelation function induced by a TBL over the full simulation surface due to an insufficient number of sources to reproduce the smallest correlation lengthscale at this frequency (about 3 cm). However, the mean square error, $J_e = 10 \log_{10} \left\{ \frac{\text{Tr}[(\mathbf{I} - \mathbf{G}\mathbf{G}^\dagger)\mathbf{S}_{dd}]}{\text{Tr}[\mathbf{S}_{dd}]} \right\}$, decreases from -0.8 dB down to -5 dB if the TBL synthesis is focused over a quarter of the initial surface, thereby improving the accuracy with which the correlation function is reproduced. In the wavenumber domain, Figure 2 (right) shows that a regular TBL synthesis using 8×8 sources is only able, in the best case, to reproduce at 1 kHz the large spatial lengthscales linked to the acoustic wavenumber, $k_0 = 18.5 \text{ m}^{-1}$, along the flow direction. But a focused TBL synthesis moves the energetic spot towards the convective wavenumber, $k_c = 30.7 \text{ m}^{-1}$, linked to sub-wavelength scales.

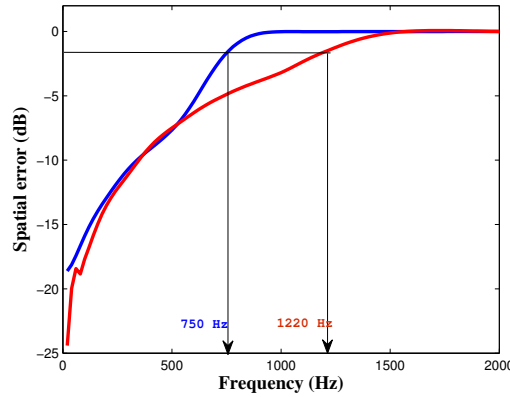


Figure 3: Variations with frequency of the spatial error with which a high-speed subsonic TBL is reproduced using an array of 8×8 sources: regular (blue) and focused (red) synthesis

Figure 3 shows that below 600 Hz, both the regular and focused synthesis approaches reproduce a TBL with a similar spatial accuracy, quantified by the spatial error, $\varepsilon_e = 10 \log_{10} \left\{ \left\| \mathbf{G} \mathbf{W}_{\text{opt}} \mathbf{W}_{\text{opt}}^H \mathbf{G}^H - \mathbf{S}_{dd} \right\| / \left\| \mathbf{S}_{dd} \right\| \right\}$. However, a focused approach extends up to 1.3 kHz the frequency with which a TBL can be synthesized with an acceptable accuracy ($\varepsilon_e < -2$ dB). This is in accordance with the theoretical criterion [10],

$$f_{\max} = U_c \sqrt{\frac{N_x^{\text{HP}} N_y^{\text{HP}}}{9.18 S}}, \quad (4)$$

with N_x^{HP} (resp. N_y^{HP}) the number of sources along the spanwise (resp. streamwise) directions and S the area of the simulation surface.

3 Reduced-rank synthesis

3.1 Parsimonious representation of the target CSD

This approach aims at synthesizing a reduced-rank approximation \mathbf{S}_{dd}^N of order N of \mathbf{S}_{dd} . It is based on the eigendecomposition $\mathbf{S}_{dd} = \mathbf{Q} \mathbf{\Lambda} \mathbf{Q}^H$ with \mathbf{Q} the matrix of eigenmodes and $\mathbf{\Lambda}$ the matrix whose diagonal elements are the eigenvalues of \mathbf{S}_{dd} . \mathbf{S}_{dd}^N then reads $\mathbf{S}_{dd}^N = \mathbf{Q}_N \mathbf{\Lambda}_N \mathbf{Q}_N^H$ with \mathbf{Q}_N (resp. $\mathbf{\Lambda}_N$) sub-matrices of \mathbf{Q} (resp. $\mathbf{\Lambda}$) truncated at N columns (resp. N columns and N rows). The optimum matrix of control filters for a reduced-rank synthesis of order N is then given by $\mathbf{W}_{\text{opt},d}^N = \mathbf{G}^\dagger \mathbf{Q}_N \sqrt{\mathbf{\Lambda}_N}$.

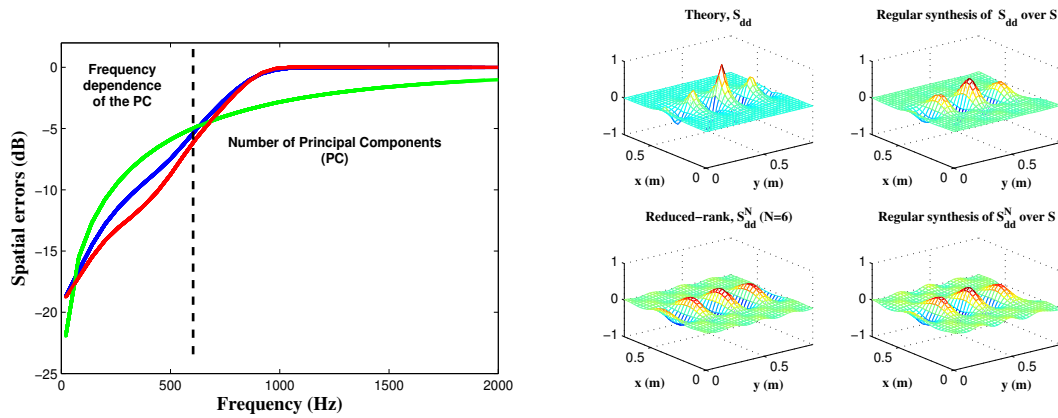


Figure 4: (Left) variations with frequency of the spatial error with which a high-speed subsonic TBL is reproduced using an array of 8×8 sources: regular synthesis (blue), synthesis of the reduced-rank approximation S_{dd}^N ($N = 6$, red) and approximation error (green); (right) spatial effect of a regular synthesis of S_{dd}^N ($N = 6$) at 800 Hz.

Figure 4 (left) shows that synthesizing the contribution of the first 6 Principal Components (PCs) of a TBL provides a spatial error of the same order as a regular synthesis of S_{dd} . Indeed, the PCs are frequency-dependent and their spatial lengthscales decrease with frequency so that the effort for a reduced-rank synthesis is mostly limited, below 600 Hz, by the ability of the source array to reproduce such reduction in the CPs wavelengths, and above 600 Hz, by the number of CPs to be accounted for because the eigenvalues then tend to be close to each other. It can be seen from Figure 4 (right) that a reduced rank approximation to a TBL CSD is reproduced at 800 Hz with the same spatial accuracy ($\epsilon_e \approx -2$ dB) as a full TBL when using a near-field array of 8×8 sources. Hence, synthesizing a reduced-rank approximation of a TBL does not seem to extend the frequency range of the simulation. This is not due to the reduced-rank approximation since the error quantifier (green curve in Fig. 4, left) stays below -3 dB up to 2 kHz.

3.2 Parsimonious filtering of the source-field transfers

On top of the number of sources required to reproduce the spatial decay of the correlation lengths with frequency, another limiting factor is the spatial filtering caused by the acoustical transfers to be equalized between the sources and the microphones. This low-pass filtering is shown in Figure 5 by a plateau-like distribution of the singular values of the source-field transfer matrix \mathbf{G} , that steeply decay for orders higher than 10 at 800 Hz. In order to relax the constraint on the required number of sources for a TBL synthesis, it is of interest to equalize only the principal source-field transfer paths associated to the highest singular values of \mathbf{G} .

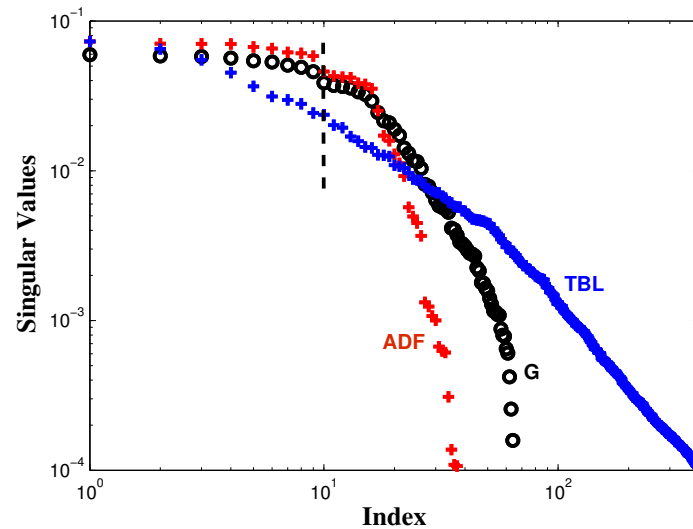


Figure 5: Decay at 800 Hz of the singular values of \mathbf{G} (black), \mathbf{S}_{dd}^{ADF} (red) and \mathbf{S}_{dd}^{TBL} (blue)

This approach is based on a singular value decomposition of \mathbf{G} that reads $\mathbf{G} = \mathbf{U}\mathbf{\Sigma}\mathbf{V}^H$ where \mathbf{U} (resp. \mathbf{V}) are the matrices of the singular field (resp. source) modes and $\mathbf{\Sigma}$ the rectangular diagonal matrix constituted of $N_{HP} = 64$ singular values along its main diagonal, if one assumes an array of 8×8 sources for the synthesis.

The synthesis of either an Acoustic Diffuse Field (ADF) or a TBL is considered. Figure 5 shows that the low-pass filtering induced by the source-field acoustical transfers at 800 Hz does not restrain the number of Degrees Of Freedom (DOFs) of an ADF, but this is not the case for a TBL. Therefore, it is expected that the equalization of the 10 first principal transfers (shown as a dashed vertical line in Fig. 5) will limit the accuracy with which a TBL is reproduced, but not the one associated to an ADF synthesis.

This is verified in the Figure 6 below in which the equalization of \mathbf{G}_{10} provides an accurate ADF reproduction with a spatial error of -4 dB. However, the equalization of \mathbf{G}_{10} induces an important truncature of the numbers of DOFs required for a TBL reproduction. Of interest is that the truncature of spatial scales larger or equal to the acoustic wavelength leads to the synthesis of a sinc-like correlation function similar to the one associated to an ADF. An equalization of \mathbf{G}_{30} would be required to recover a reproduction accuracy similar to the one induced by a regular TBL synthesis.

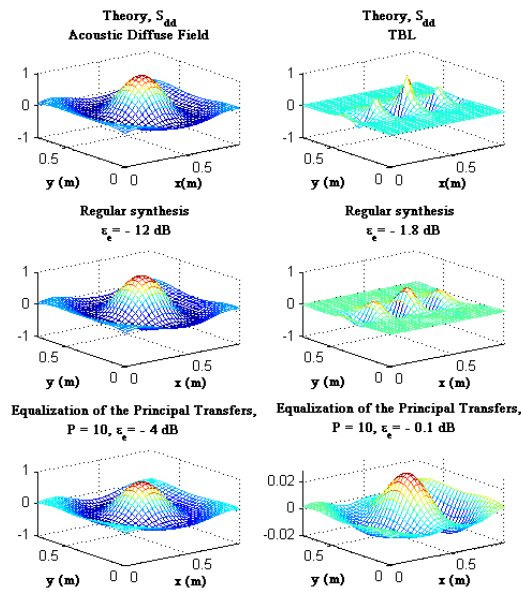


Figure 6: Equalization of the 10 source-field Principal Transfers and its effect on the synthesis of an ADF and a TBL at 800 Hz using a near-field array of 8×8 sources.

4 Conclusions

Three approaches have been compared in order to extend the frequency range over which a subsonic TBL may be synthesized while keeping a reasonable number of reproduction sources.

- Focused synthesis of the TBL wall-pressures over a reduced simulation domain $S_f < S$ extends the upper frequency up to which a TBL can be accurately synthesized by a ratio $0.8\sqrt{S/S_f}$. If one considers a reduced simulation surface of size $S_f = 0.2 \times 0.17 \text{ m}^2$, similar to that of an aircraft fuselage panel comprised between two circumferential stiffeners and longitudinal frames [6], the maximum frequency for a TBL simulation with a near-field array of 8×8 sources could be extended up to 2680 Hz. These predictions are being verified experimentally in the LMA semi-anechoic room using a 64 channel arbitrary waveform generator and a modular baffled array of 8×8 loudspeakers.
- Synthesis of the first principal components of a TBL does not upshift the maximum frequency that can be reached for a regular synthesis of the TBL. Indeed, synthesizing the first principal components rapidly requires a number of sources able to cope with the decrease in the PC sub-wavelength scales, as it is the case for a regular synthesis.
- The synthesis of wall-pressures through equalization of the first source-field acoustical transfers is recommended when the target random process is band-limited with a cut-off

wavenumber lower than the one associated to the source-field acoustical transfers. This is the case for an ADF, but not for a TBL.

Acknowledgments

This study was part of the BLOWING project funded by the Spanish Ministry of Economy and Competitiveness (TRA2014-56639-R, 2015-2017).

References

- [1] Fahy, F. J.; On simulating the transmission through structures of noise from turbulent boundary layer pressure fluctuations, *Journal of Sound and Vibration* **3**, 57-81 (1966).
- [2] Dodds, C. J. The laboratory simulation of vehicle service stress, *ASME Journal of Engineering for Industry* **96**, 391-398 (1974).
- [3] Robert, G.; Sabot, J. Use of random forces to simulate the vibroacoustic response of a plate excited by a hydrodynamic turbulent boundary layer, *Proceedings of the ASME Winter Meeting: Symposium on Flow-Induced Vibrations* **5**, 53-61, 1984.
- [4] Steinwolf, A.; White, R. G.; Wolfe, H. F. Simulation of jet-noise excitation in an acoustic progressive wave tube facility, *Journal of the Acoustical Society of America* **109**, 1043-1052 (2001).
- [5] Gauthier, P. A.; Camier, C.; Gauthier, O.; Pasco, Y.; Berry, A. Aircraft sound environment reproduction: Sound field reproduction inside a cabin mock-up using microphone and actuator arrays, *Proceedings of Meetings in Acoustics, International Congress on Acoustics ICA 2013, Array Signal Processing for Three-Dimensional Audio Applications I*, Montreal, Canada; June 2-7, **19**, paper 055008, 2013.
- [6] Wilby, J. F.; Gloyna, F. L. Vibration measurements of an airplane fuselage structure I. turbulent boundary layer excitation, *Journal of Sound and Vibration* **23**, 443-466 (1972).
- [7] Bhat, W. V. Flight test measurements of exterior turbulent boundary layer pressure fluctuations on Boeing model 737 airplane, *Journal of Sound and Vibration* **14**, 439-457 (1971).
- [8] Maury, C.; Elliott, S. J.; Gardonio, P. 2004, Turbulent boundary layer simulation with an array of loudspeakers, *AIAA Journal*, **42**, 706-713 (2004).
- [9] Bravo, T.; Maury, C. The experimental synthesis of random pressure fields: Methodology, *Journal of the Acoustical Society of America* **120**, 2702-2711 (2006).
- [10] Maury, C.; Bravo, T. The experimental synthesis of random pressure fields: Practical feasibility, *Journal of the Acoustical Society of America* **120**, 2712-2723 (2006).
- [11] Bravo, T.; Maury, C. A synthesis approach for reproducing the response of aircraft panels to a turbulent boundary layer excitation, *Journal of the Acoustical Society of America* **129**, 143-153 (2011).
- [12] Berry, A.; Dia, R.; Robin, O. A wave field synthesis approach to reproduction of spatially-correlated sound fields, *Journal of the Acoustical Society of America* **131**, 1226-1238 (2012).
- [13] Robin, O.; Berry, A.; Moreau, S. Reproduction of random pressure fields based on planar nearfield acoustic holography, *Journal of the Acoustical Society of America* **133**, 3885-3899 (2013).
- [14] Aucejo, M.; Maxit, L.; Guyader, J.-L. Experimental simulation of turbulent boundary layer induced vibrations by using a synthetic array, *Journal of Sound and Vibration* **331**, 3824-3843 (2012).
- [15] Corcos, G. M. Resolution of pressure in turbulence, *Journal of the Acoustical Society of America* **35**, 192-199 (1963).